3D Discrete element approach to the problem on abutment pressure in a gently dipping coal seam

S V Klishin and A F Revuzhenko

Chinakal Institute of Mining, Siberian Branch of the Russian Academy of Sciences, 54 Krasnyi pr., Novosibirsk, 630091, Russia

E-mail: sv.klishin@gmail.com

Abstract. Using the discrete element method, the authors have carried out 3D implementation of the problem on strength loss in surrounding rock mass in the vicinity of a production heading and on abutment pressure in a gently dripping coal seam. The calculation of forces at the contacts between particles accounts for friction, rolling resistance and viscosity. Between discrete particles modeling coal seam, surrounding rock mass and broken rocks, an elastic connecting element is introduced to allow simulating coherent materials. The paper presents the kinematic patterns of rock mass deformation, stresses in particles and the graph of the abutment pressure behavior in the coal seam.

1. Introduction

Abutment pressure in a gently dipping coal seam is represented by normal compressive stresses affecting the seam along its length and generated under re-distribution of stress state by a discontinuity in rock mass. Abutment pressure is created by the weight of the overlying strata in combination with the sum of bending moments of rocks above a mined-out void or another cavity [1 - 5].

Abutment pressure induces diverse processes in rocks that impose serious threat to mining. Unexpected and uncontrollable dynamic rock falls are highly harmful for miners, machines and excavations. Furthermore, roof overhangs create concentrated ground pressure on coal in the zone of production headings and junctures with roadways, which provokes rockbursting. Under such conditions, pillars and supported development headings also experience high abutment pressure due to roof overhang over large areas.

Despite appreciable advance in the description of the abutment pressure events, selection of the most adequate characterization of the post-limit rock mass behavior in the boundary value problems on rock stability and failure in underground mines yet presents a difficulty [6 - 8].

Figure 1 depicts the problem to be discussed in this paper. Let rock mass (*1*) contain a gently dipping coal seam (*2*) with a thickness h_c and caved roof rocks (*3*) at a depth of h_m from the free surface (*5*). The contour of a heading (*4*) is free from normal and shear stresses. The main approach to solving this problem is based on the theory of plasticity and elasticity and uses the finite element method. The boundary conditions in the considered domain are governed by the initial stress state of rock mass in the field of gravity. Many researchers describe these conditions using Dinnik's hypothesis. Usually, conditions of continuous stresses and displacements are assumed at the interfaces of enclosing rocks, caved rocks and coal seam. The elastic and elastoplastic models use, as a rule, geometrically linear formulations of problems. For this reason, displacements are assumed small. This constraint is essential and not always conformable with a real situation.

The two-dimensional model of rock mass constructed in [8] based on the concept of rock as a medium with the internal sources and sinks of energy took into account block structure, anisotropic properties, inter-block sliding and strength loss in rock mass. The model was used to solve the problem on deformation of a rock pillar. The authors described successive development of zones of local strength loss and residual strength. The effect of unstable deformation was demonstrated in the form of development of long narrow bands of shearing that can result in disastrous failure of a pillar.

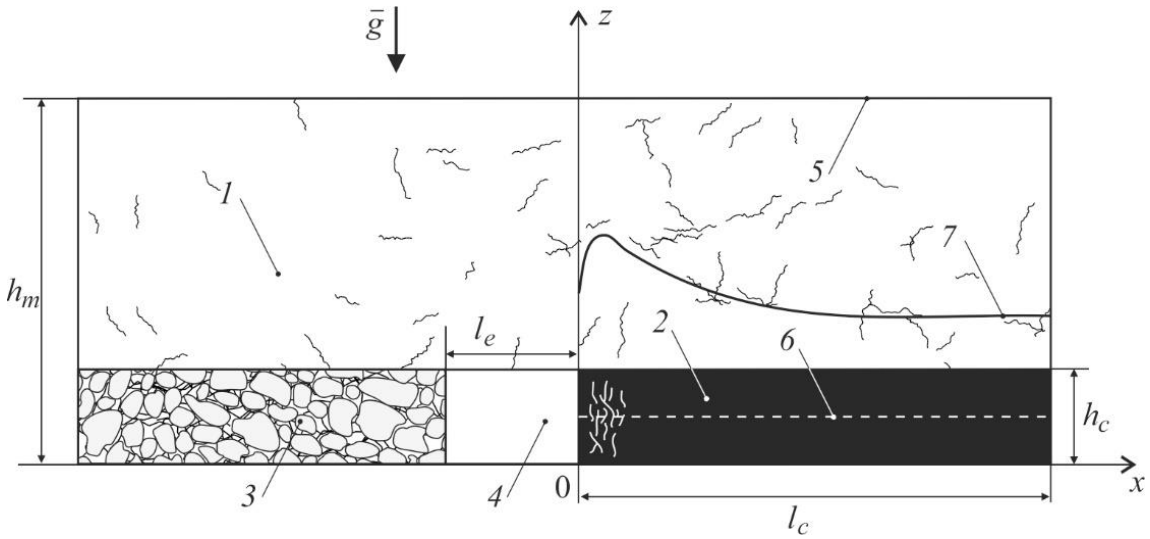

Figure 1. Analytical model of mining: 1 – enclosing rocks; 2 – coal seam; 3 – caved rocks; 4 – production heading; 5 – free surface; 6 – central cross section of the seam to measure abutment pressure; 7 – epure of abutment pressure distribution.

To study large deformations, it seems sufficiently adequate to use an approach based on the discrete element method (DEM). This method enables determining evolution of stress state in rocks both at the pre-limit stage of loading and at the stage of transition to localization of shearing and failure. Introduced in [9], DEM currently is widely popular and used to solve many geomechanical problems [10–12]. In this method, a real medium is replaced by a package of discrete particles with the certain interaction conditions assumed at the particle contacts. Most researches use spherical discrete elements with the pre-set distribution of radii. This method involves no difficulties when solving problems on large (finite) deformations and rotations. Thus, DEM is the main alternative to the classical methods based upon conventional provisions of continuum mechanics.

2. Discrete element method

In accordance with DEM, a medium to be studied is represented as a package of N spherical particles (discrete elements). Each i-th element possesses a radius r_i and the known set of physical and contact properties of the particle material: density, elastic and viscous moduli, friction, cohesion etc. ($i = 1, \ldots, N$). Motion of a discrete element is composed of translation and rotation and is given by the equations below:

$$m_i \ddot{\mathbf{x}}_i = \sum_j \boldsymbol{f}_{ij} + m_i \boldsymbol{g}\,, \tag{1}$$

$$I_i \ddot{\boldsymbol{\theta}}_i = \sum_j (\mathbf{r}_{ic} \times \boldsymbol{f}_{ij} + \boldsymbol{M}_{r,ij})\,. \tag{2}$$

Here, points imply differentiation with respect to time t; $\boldsymbol{x}_i$ is the radius-vector of the center of gravity of an i-th particle; $\boldsymbol{\theta}_i$ is the turn of the i-th particle relative to the coordinate axes; m_i and I_i are the mass and inertia moment of the i-th particle, respectively; $\boldsymbol{g}$ is the acceleration of gravity; $\boldsymbol{r}_{ic}$ is the vector from the center of the i-th particle to the contact point; $\boldsymbol{f}_{ij}$ is the contact force applied to the i-th

particle by a *j*-th particle (or boundary), depends on the overlapping of the particles, as well as on the elastic and viscous moduli; $\boldsymbol{M}_{r,ij}$ is the rolling resistance moment of the *i*-th and *j*-th particles (or boundary). Summation in (1) and (2) is carried out with respect to all elements and boundaries that contact the *i*-th particle. It is assumed that discrete elements preserve their shape for the period of contact; for this reason, the degree of their deformation is only described by the value of overlap between the particles in contact.

The contact force between particles is calculated from the Kelvin–Voigt viscoelastic model that accounts for normal and shear components. This model is schematically depicted in figure 2a. The normal component of the contact force is found using the Hertz law [13], and the shear component is calculated from the scheme by Mindlin and Deresiewicz [14 - 15].

Since rocks are a cohesive material capable to accumulate and release elastic energy, the described deformation model should be added with a connecting element between the particles in contact. This connecting element is introduced in the model in the form of extra forces (elastic springs) of pre-set stiffness, which prevent separation of the contact elements (figure 2b).

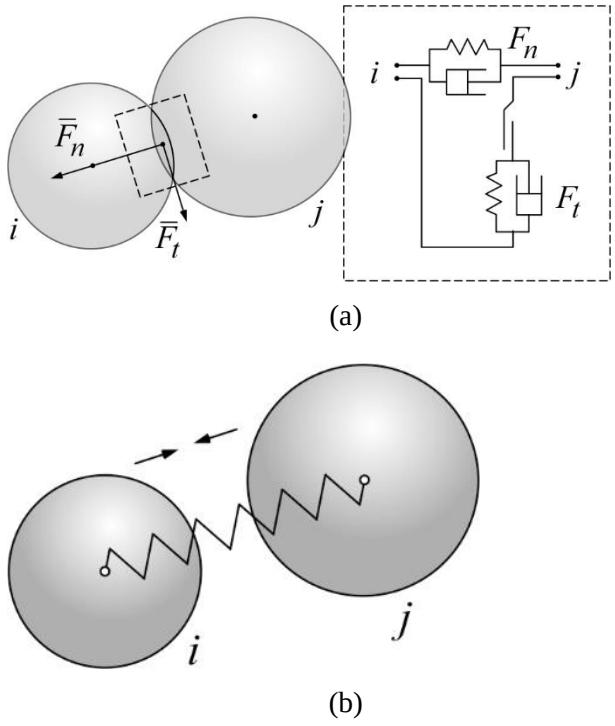

Figure 2. (a) Schematic interaction of particles based on the rheological Kelvin–Voigt model; (b) connecting elements between discrete particles composing intact rock mass.

3. Numerical experiment

Having the data on the law of motion and interaction of particles, i.e. Eqs. (1) and (2), as well as initial and boundary conditions, it is possible to solve the equations and determine evolution of stress state in a medium. The Chinakal Institute of Mining has developed DEM-based software for the numerical analysis of motion modes in granular materials composed of individual spherical particles [16, 17].

Figure 3 presents the scheme of the 3D numerical experiment. The objective domain is presented by a package of $N = 150\,000$ discrete elements having radii selected from a uniform distribution between 0.025 and 0.05 m. The particles fill a domain in the form of a parallelepiped with a length of 34 m, height of 18 m and width of 1 m along the axes *Ox*, *Oz* and *Oy*, respectively. The sides *AB* and *CD*, and the faces oriented in parallel to the coordinate plane *Oxz* are perfectly smooth. At the upper boundary *AD* the pressure F_z is set in conformity with the mining depth of 300 m. The recovery factor for the velocity between particles, describing dissipation of energy upon the particle collision, equals 0.65. The table below (table 1) describes the physical parameters of the elements composing the coal seam (*1*), rock mass (*2*) and caved area (*3*). The initial package of untouching particles was subjected to settlement under the force of gravity with regard to contact interaction. Upon reaching the equilibrium, elastic nondestructive connections (spring) with the stiffness of 10 MPa were created between the particles being in contact. The connections between the discrete elements representing coal and enclosing rocks are uniformly spread in the volume, while the connections between the particles in the caved area are created within a mesh of cubic cells 0.5×0.5×0.5 m, with formation of separate blocks.

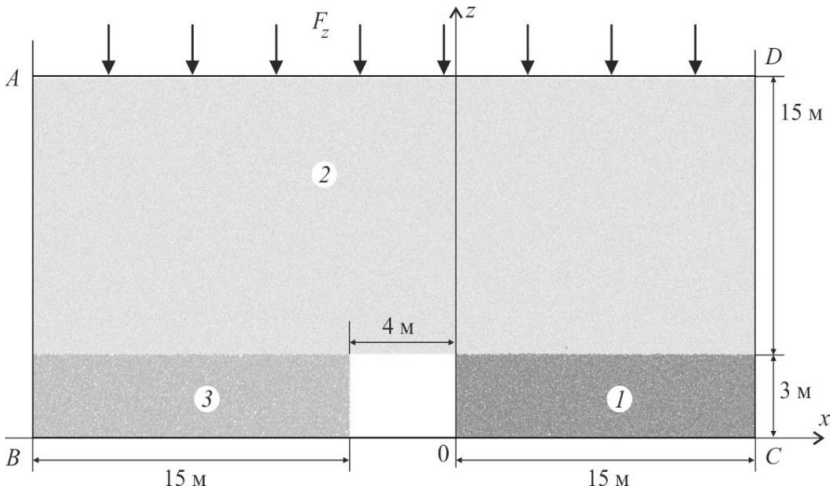

Figure 3. DEM-based experiment scheme.

Table 1. Physical parameters of particles.

	Coal	Rock mass	Caved rocks
Elasticity modulus, MPa	$5 \cdot 10^3$	$1.5 \cdot 10^4$	$1.5 \cdot 10^4$
Poisson's ratio	0.16	0.25	0.25
Density, kg/m	1300	2400	2400

The external dry friction angle φ_{ij} varies from 26 to 33° for the test materials. The present studies use φ_{ij}= 30°. Selection of the rolling resistance angle ψ_{ij}, having large influence on the contact interaction and relative rotations of discrete elements, needs additional numerical experimentation. The specified parameter is determined as follows. In Eq. (2) the moment upon the contact of two particles is represented as two summands. The first summand is a moment that appears under relative sliding of particles over one the other given dry friction is present. The second summand is a moment that impedes relative rotation of discrete elements:

$$\boldsymbol{M}_{r,ij} = -\frac{\boldsymbol{\omega}_i - \boldsymbol{\omega}_j}{\left|\boldsymbol{\omega}_i - \boldsymbol{\omega}_j\right|} \mu_{ij} r_{ij} \left| \boldsymbol{f}_{ij} \cdot \boldsymbol{n}_{ij} \right|, \tag{3}$$

where $\boldsymbol{\omega}_i$ and $\boldsymbol{\omega}_j$ are the angular velocities of the contact particles; $\boldsymbol{n}_{ij}$ is the unit vector lying in the straight line between the centers of the contact particles; r_{ij} is the reduced radius:

$$\frac{1}{r_{ij}} = \frac{1}{r_i} + \frac{1}{r_j}.$$

The dimensionless parameter μ_{ij} is the rolling resistance coefficient. By analogy with the dry friction angle between two bodies, it is readily shown that $\mu_{ij} = \operatorname{tg} \psi_{ij}$ [18]. The angle of rolling resistance is the maximum slope of a plane, at which a spherical particle occurs in this plane in the equilibrium condition under the action of gravity.

The authors have carried out a test experiment on numerical determination of slope of granular material in the three-dimensional formulation (figure 4). Particles were placed in a parallelepiped box with the perfectly smooth walls (figure 4a). When the particles reached equilibrium, the side walls of the box were moved upwards at a constant low velocity. The particles showered from the box and were withdrawn from the calculations. By the end of the experiment, the granular medium acquired

the triangular form as in figure 4b. The tests were performed for the constant dry friction angle φ_{ij}= 30° and varied angles of rolling resistance. It is seen that the latter has an essential influence on the formation of slopes of the granular material. Based on the calculated data, the rolling resistance angle was selected for all media as ψ_{ij}= 15°.

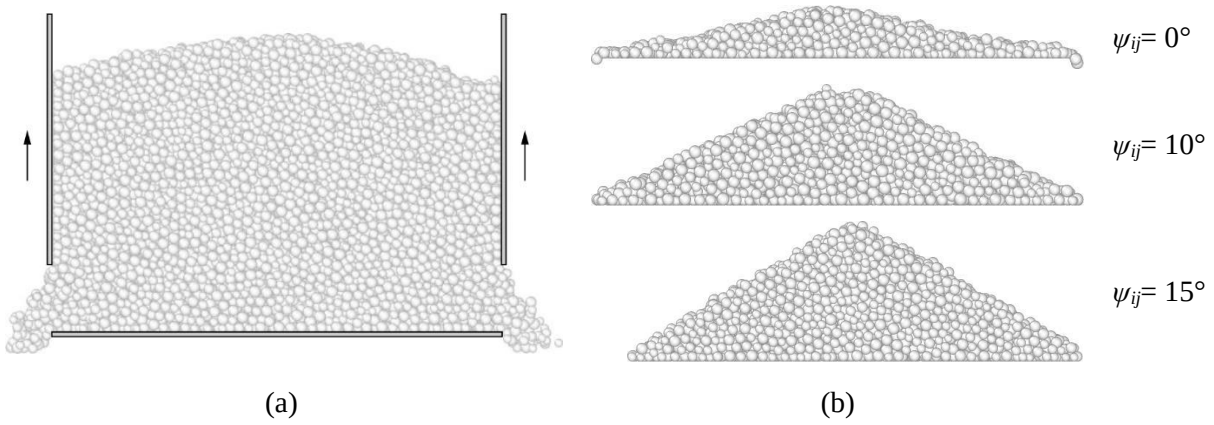

Figure 4. Numerical experiment to find natural slope of granular material at different rolling resistance angles ψij and constant dry friction angle φij= 30°: (a) schematic of the experiment; (b) final configuration of material.

Turn back to the problem. At the upper boundary *AD* of the initially equilibrium medium (figure 3), we assign the vertical pressure F_z that gradually increases in value from zero until pressure conformable with the mining depth of 300 m. Figure 5 depicts the state of the medium under deformation at the final stage of loading. It is seen that as a consequence of the zero boundary conditions at the contour of the heading, squeezing of edge coal towards the heading takes place, and high subsidence of the heading roof is visible. The blocks composing the caved material deform under the weight of the overlying rocks and fall in the mined-out area.

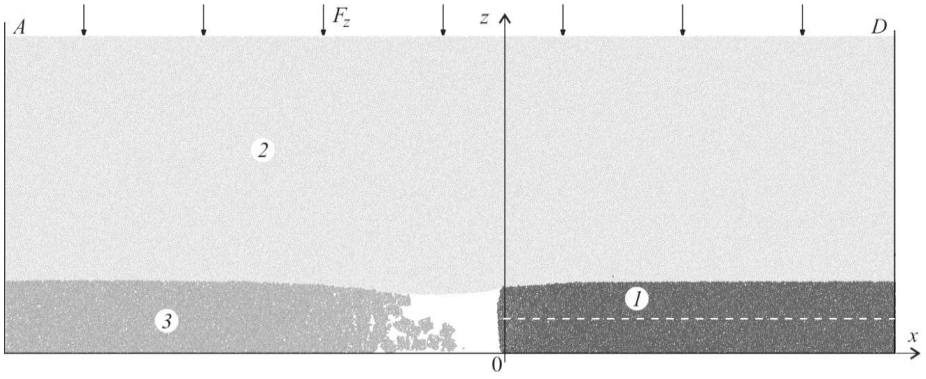

Figure 5. State of the medium at the last stage of deformation.

The distribution of horizontal and vertical stresses in discrete elements is illustrated in figure 6. Here, particles having higher compression modulus are shown by the darker color, and the particles with the lower compression modulus — by the lighter color.

In the epure of abutment pressure in a coal seam in figure 7, the vertical compressive stresses on the particles in the central cross section (refer to figure 5) are shown. It is seen that the peak pressure is at the distance of 0.5 to 2 m from the face breast.

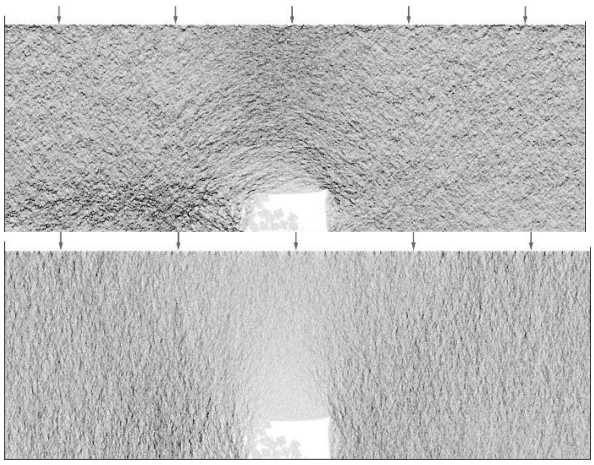

Figure 6. Distribution of (top) horizontal and (bottom) vertical stresses in the particles at the end of loading.

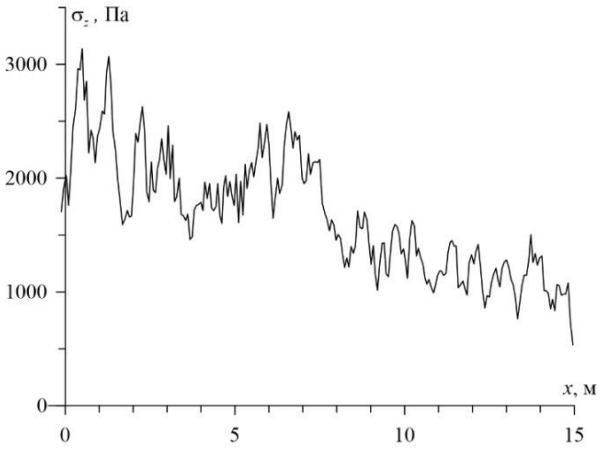

Figure 7. Vertical stresses on the particles in the central cross section of coal seam.

4. Conclusion

It seems the most appropriate to study problems on abutment pressure events in gently dipping coal seams using the discrete element method for its allows accounting for large deformations and rotations. The introduction of additional connections in the form of elastic potentials between particles enables describing the field of finite deformation during interaction of gently dipping coal seams and enclosing rock mass as well as the fall of broken rocks in roadways.

Acknowledgements

The study has been supported by the Russian Science Foundation, Project No. 16-17-10121.

References

[1] Gritsko G I, Vlasenko B V and Posokhov G E et al 1980 *Prediction and Calculation of Rock Pressure Events* (Novosibirsk: Nauka)
[2] Borisov A A, Matantsev V I, Ovcharenko B P and Voskoboev F N 1983 *Ground Control* (Moscow: Nedra)
[3] Ardashev K A, Krylov V F and Kuksov N I et al 1967 *Improvement of Ground Control in Mining Inclined and Steeply Dipping Seams* (Moscow: Nedra)
[4] Bieniawski Z T 1987 *Strata Control in in Mineral Engineering* (Wiley)
[5] Litvinsky G G 2000 *Proc. Int. Conf. on Propsects for Coal Industry Development at the Edge of XXI Century* (Alchevsk: DGMI) pp 72–8
[6] Pavlova L D 2006 *GIAB* **4** 57–60
[7] Kuznetsova A V and Smolin I Yu 2010 *Vestn. Tomsk Gos. Univer. Matem. Mekh.* **2(10)** 79–87
[8] Lavrikov S V and Revuzhenko A F 2014 *Calculation of Deformation and Stability of Pillars in Rocks AIP Conference Proceedings* **1623** 335
[9] Cundall P A and Strack O D L 1979 *Géotechnique* **29(1)** 47–65
[10] Klishin S V, Klishin V I and Opruk G Yu 2013 *J. Min. Sci.* **49(6)** 932–40
[11] Kramadzhyan A A et al 2015 *J. Min. Sci.* **51(6)** 1077–84
[12] Klishin S V and Revuzhenko A F 2015 *J. Fundament. Appl. Min. Sci.* **2(1)** 235–9

[13] Johnson K 1985 *Contact Mechanics* (Cambridge University Press)
[14] Mindlin R D 1949 *J. Appl. Mech.* **16** 259–68
[15] Mindlin R D and Deresiewicz H 1953 *J. Appl. Mech.* **20** 327–44
[16] Klishin S V and Revuzhenko A F 2016 *Proc. Int. Sci. Conf on Knowlwdge-based Technologies in Development of Use of Mineral Resources* (Novokuznetsk: SibSIU) **2** pp 39–46
[17] Lavrikov S V and Revuzhenko A F 2016 *J. Min. Sci.* **52(4)** 632–7
[18] Klishin S V and Revuzhenko A F 2015 *J. Min. Sci.* **51(5)** 1070–6